



## Glycolipid self-assembly: micellar structure

Marie-Christine Cecutti, Bonaventura Focher, Bruno Perly, Thomas Zemb

### ► To cite this version:

Marie-Christine Cecutti, Bonaventura Focher, Bruno Perly, Thomas Zemb. Glycolipid self-assembly: micellar structure. *Langmuir*, 1991, 7 (11), pp.2580-2585. 10.1021/la00059a031 . hal-02094679

**HAL Id: hal-02094679**

**<https://hal.science/hal-02094679>**

Submitted on 9 Apr 2019

**HAL** is a multi-disciplinary open access archive for the deposit and dissemination of scientific research documents, whether they are published or not. The documents may come from teaching and research institutions in France or abroad, or from public or private research centers.

L'archive ouverte pluridisciplinaire **HAL**, est destinée au dépôt et à la diffusion de documents scientifiques de niveau recherche, publiés ou non, émanant des établissements d'enseignement et de recherche français ou étrangers, des laboratoires publics ou privés.




## Open Archive Toulouse Archive Ouverte (OATAO)

OATAO is an open access repository that collects the work of Toulouse researchers and makes it freely available over the web where possible

This is an author's version published in: <http://oatao.univ-toulouse.fr/23551>

**Official URL:** <https://doi.org/10.1021/1a00059a031>

### **To cite this version:**

Cecutti, Marie-Christine  and Focher, Bonaventura and Perly, Bruno and Zemb, Thomas *Glycolipid self-assembly: micellar structure*. (1991) *Langmuir*, 7 (11). 2580-2585. ISSN 0743-7463

Any correspondence concerning this service should be sent  
to the repository administrator: [tech-oatao@listes-diff.inp-toulouse.fr](mailto:tech-oatao@listes-diff.inp-toulouse.fr)

# Glycolipid Self-Assembly: Micellar Structure

Christine Cecutti,<sup>\*,†</sup> Bonaventura Focher,<sup>‡</sup> Bruno Perly,<sup>§</sup> and Thomas Zemb<sup>§</sup>

*Ecole Nationale Supérieure de Chimie de Toulouse, 118 route de Narbonne, F.31077 Toulouse cedex, France, C.N.R., P.zza L. da Vinci, I.20133 Milano, Italy, and CEA-CEN de Saclay, Service de Chimie Moléculaire, F.91191 Gif sur Yvette cedex, France*

Small-angle scattering is used to investigate a typical glycolipid micelle structure in conjunction with NMR determination of sugar cycle conformation. It is shown that the ellipsoidal shape of the micelle originates from two constraints: sugar rings perpendicular to the interface induce a limited area at the chain-head interface. Together with the bulky hydrated heads, this imposes an ellipsoidal shape.

## Introduction

Single-chain surfactants are usually classified into two families: ionic and nonionic molecules. In the phase diagram, a diluted, optically isotropic fluid micellar phase  $L_1$  exists for both types of surfactants. The micellar structure, i.e., the number of water molecules bound per headgroup, the radius of the micellar hydrophobic core, and the area per surfactant head, is determined by geometric constraints<sup>1</sup> and by the balance between headgroup repulsion and hydrophobic effects between apolar chains. In the case of most ionic single-chain molecules without added salt, the size and structure of the aggregates in micellar phase is roughly independent of concentration and temperature at any point of the phase diagram far from the phase limits. Nonionic micelles exhibit a sphere to rod transition in binary solutions. At increasing temperature, the lower consolute point is due to attractive interactions appearing between nonionic headgroups when the interfacial radius of curvature decreases.<sup>2</sup> Typical values of the physical quantities describing these two types of micelles, including the microstructural parameters, are given in Table I for two classical examples: 2% SDS in  $D_2O$  and 5% C12E5 in  $D_2O$  at room temperature.

We examine here the case of a biologically important molecule,  $\beta$ -dodecyl maltoside. This is a nonionic molecule with an extremely large hydrophilic headgroup. We first want to assess the following questions: as the large headgroup gives rise to a large sterical repulsive term, will this be sufficient to induce the characteristic structure of ionic micelles, with some particularities such as the absence of a salt effect due to the absence of counterions? On the other hand, will glycolipid micelles present the same phase behavior and microstructure as other nonionic systems?

Our aim in this work is to identify the dominant features of glycolipid self-assembly in the micellar state using  $\beta$ -dodecyl maltoside ( $\beta$ C12M) as a typical molecule.  $\beta$ C12M presents a large and flexible headgroup made by two sugar rings. Therefore, after identification of the phases in a binary concentration and temperature phase

**Table I. Typical Molecular Parameters for the Ionic Surfactant Sodium Dodecyl Sulfate (SDS), the Nonionic Polyethylene (C12E5), and  $\beta$ -Dodecyl Maltoside ( $\beta$ C12M)**

	SDS	C12E5	$\beta$ C12M
$V_{\text{mol}}$ , nm <sup>3</sup>	0.380	0.620	0.691
headgroup areas $\sigma$ , nm <sup>2</sup>	0.70	0.35	0.50
headgroup areas $\sigma'$ , nm <sup>2</sup>	0.60	0.35	
chain length $l$ , nm	1.8	1.8	1.8
packing parameter, $V_{\text{mol}}/\sigma l$	0.3	1.0	0.75
volume of headgroup, nm <sup>3</sup>	0.060	0.300	0.376

diagram, we studied the sugar ring conformation by NMR and the micellar structure by X-ray and neutron scattering.

The same methods have been used for other surfactants with a bulky nonionic headgroup.<sup>3,4</sup> With a mixture of lipopolysaccharides isolated from *Escherichia coli*, with an average of four sugar rings per molecule,<sup>3</sup> long cylinders, similar to those obtained with diheptanoylphosphatidylcholine<sup>5</sup> with a pH-dependent length have been evidenced. Nonspherical micelles have been obtained with the ganglioside GM1.<sup>4</sup>

## Materials and Methods

**(1) Scattering Techniques.** X-ray small-angle scattering of isotropic phases has been performed on the D24 double-crystal diffractometer in Lure (Orsay), using a wavelength of 0.122 nm and a sample to detector distance of 59.3 cm. The results were identical using deuterated and protonated octane as solvent. The obtained  $q$  range was  $q_{\text{min}} = 0.03 \text{ nm}^{-1}$  and  $q_{\text{max}} = 6 \text{ nm}^{-1}$ ; i.e., the resolution was  $2\pi/q_{\text{max}} = 1 \text{ nm}$  and no long-range ordering higher than  $2\pi/q_{\text{min}} = 200 \text{ nm}$  was considered. The absolute scaling was made by comparison with the isotropic coherent scattering<sup>6</sup> of a sample of 1.5-mm thickness of water between 25- $\mu\text{m}$  thick Mylar sheets. Due to water compressibility, each water molecule gives the same uniform scattering as 6.35 independent electrons. This type of normalization, versus a very weak but constant signal, ensures that the setup is perfectly aligned and that background correction is successfully achieved.<sup>7</sup> Neutron small-angle scattering was performed on the PACE setup at LLB Orphée, using 0.5–1-nm wavelengths with two different wavelengths, which gives a  $q$  range of  $q_{\text{min}} = 0.08 \text{ nm}^{-1}$  to  $q_{\text{max}} = 3 \text{ nm}^{-1}$ . Absolute scaling

<sup>\*</sup> Ecole Nationale Supérieure de Chimie de Toulouse.

<sup>†</sup> C.N.R.

<sup>‡</sup> CEA-CEN de Saclay.

(1) Israelachvili, J. N.; Mitchell, D. J.; Ninham, B. W. *J. Chem. Soc., Faraday Trans. 2* 1976, 72, 1525.

(2) Mitchell, D. J.; Tiddy, G. J.; Waring, L.; Bostock, T.; McDonald, M. P. *J. Chem. Soc., Faraday Trans 1* 1983, 79, 975.

(3) Hayter, J. B.; Rivera, M.; McGroarty, E. J. *J. Biol. Chem.* 1987, 262, 5100.

(4) Cantu, L.; Corti, M.; Degiorgio, V.; Piazza, R.; Rennie, A. *Prog. Colloid Polym. Sci.* 1988, 76, 218.

(5) Lin, T. L.; Chen, S. H.; Gabriel, N. E.; Roberts, M. F. *J. Phys. Chem.* 1987, 91, 406.

(6) Zemb, T.; Charpin, P. *J. Phys.* 1985, 46, 249.

(7) Levelut, A. M. *Science Phys. Thesis*, Orsay, 1968; p 334.

was made using the incoherent scattering of water.<sup>8</sup> Lyotropic liquid-crystal identification was done using a Guinier camera equipped with a linear detector, giving a  $q_{\min} = 0.2 \text{ nm}^{-1}$  to  $q_{\max} = 8 \text{ nm}^{-1}$ . The lyotropic liquid crystals were identified by peak spacing. After identification of the symmetry, the area per molecule was derived from measurement of the molecular volumes by densitometry.

The small-angle scattering of micellar solutions was first checked by the measurement of the invariant  $Q^*$ , which is given in a system with two scattering length densities  $b_1$  and  $b_2$ , with the volumes  $\phi_1$  and  $\phi_2$ :<sup>9</sup>

$$Q^* = 2\pi(b_1 - b_2)^2\phi_1\phi_2 = \int_0^{q_{\max}} i(q)q \, dq$$

This expression is valid whatever the microstructure of the solution, isolated spheres, connected cylinders, or random bilayers;<sup>10</sup> the only underlying assumption is that it is a two-medium structure. Then, the shape of the micelles has to be determined by comparing the scattering  $I(q)$  obtained with the scattering of model structures. Since the presence or absence of intermicellar attraction or repulsion is not known a priori, determination of the radius of gyration has no physical meaning. The determination of the micellar shape can only rely on a complete calculation on an absolute scale of the scattering curve for different ideal model shapes of the micelle. Fortunately, in binary solutions, micellar radii and scattering lengths are known; they are imposed by chemical composition and molecular volumes. There is no free parameter adjustment except aggregation number, itself related to the area per headgroup, once the general shape of the aggregate has been chosen, as explained below.

Our aim is to compare the shape with the surfactant parameter  $p$ , the later being deduced from steric considerations.

Usually, the volume of the polar headgroups  $V_p$  is small compared to that of the hydrophobic chains  $V_c$ . The packing parameter  $p$  is then defined as<sup>10</sup>

$$p = V_{\text{mol}}/6.1 = (V_p + V_c)/6.1 = V_c/6.1$$

In the present case, the packing of the molecule requires taking into account the whole molecular volume to evaluate to surfactant parameter. The length of the molecule is now the total length (Table I). Using the first definition,  $l = 18 \text{ \AA}$  and  $p = 0.33$  while using the total length ( $l = 24 \text{ \AA}$ ) yields also  $p = 0.33$ .

**Model of Spherical Micelles.** We suppose here that the glycolipid molecules pack into spherical droplets with hydrophobic chains inside: one single quantity, the interfacial area per molecule  $\sigma$ , determines the whole scattering spectrum:

$$I(q) = P(q)S(q)$$

The structure factor  $S(q)$  is first taken for independent hard spheres, neglecting other types of interaction.  $S(q)$  can be calculated analytically at any  $q$  with good precision when the radius  $R$  of the hard core of micelles, the density  $n$  ( $\text{cm}^{-3}$ ) of micelles, and the total volume fraction  $\phi$  of micelles are known.<sup>11</sup> These three quantities can be evaluated by molecular parameters once the area per molecule  $\sigma$  is fixed.

(a) The surface of micelles imposes a relation between  $N$  and  $R$ :

$$4\pi R^2 = N\sigma$$

where  $N$  is the aggregation number and  $\sigma$  the single adjustable parameter, which has to be between 2.5 and 7  $\text{nm}^2$  for steric reasons. Usually,  $\sigma$  is defined at the micelle-solvent interface. For typical surfactants such as SDS,  $\sigma$  is ca. 70  $\text{\AA}^2/\text{molecule}$ . It does not make any difference in this case to define  $\sigma$  at the chain-headgroup interface since the volume of the headgroup is only 10% of the total surfactant molecular volume. For glycolipids, however, the sugar rings represent the major part of the molecular volume. We therefore differentiate between the micelle-solvent interface  $\sigma$  and the hydrophobic core-sugar headgroup interface  $\sigma'$ .

(b) The micellar volume imposes another relation between  $N$  and  $R$ :

$$4/3\pi R^3 = NV_{\text{mol}}$$

where  $V_{\text{mol}}$  is the known molecular volume, measured by densitometry using the Anton Paar high-precision densitometer.

Aggregation number  $N$  and micellar radius  $R$  are now fixed:

$$N = 4\pi R^2/\sigma \quad R = 3V_{\text{mol}}/\sigma$$

The area per molecule at the core-headgroup interface is now fixed. If the shape remains spherical, the radius of the sphere including the hydrophobic chains  $R'$  is defined as

$$4\pi R'^2 = N\sigma' \quad 4/3\pi R'^3 = NV_{\text{chain}}$$

There can be a conflict between the values of  $\sigma$  and  $\sigma'$ . The aggregate shape, when nonspherical, is an energy-effective packing solution to solve this conflict.

The excluded-volume fraction  $\phi$  of the hydrated micelle is also deduced from steric considerations. The volume fraction  $\phi$  of the micelle is given by  $N$  molecular volumes including  $h = 10$  water molecules by surfactant inside the hard-sphere volume. The volume fraction  $\phi$  of the dispersed phase is therefore known a priori when  $\sigma$  is fixed:

$$\phi = (V_{\text{mol}} + h \times 30)Nn$$

Since the volume of one single water molecule is 30  $\text{\AA}^3$ , a two-step model of the micelle is sufficient to calculate the form factor  $P(q)$  in this  $q$  range:<sup>10</sup> we suppose a hydrophobic core of radius  $R_1$  and a hydrated headgroup concentric shell of radius  $R_2$ . The internal sphere of radius  $R_1$  contains only the  $N$  hydrophobic chains. The concentric shell between  $R_1$  and  $R_2$  contains  $N$  headgroups and  $hN$  water molecules. Since the molecular volumes and scattering length densities are known, the values of  $R_1$  and  $R_2$  as well as the contrast is known once  $N$  and  $h$  are fixed.  $h$  is imposed by the simulation at high volume fraction. As usual, we make the assumption that  $h$  is not concentration dependent. We found  $h = 10$  an acceptable value for this whole study. The scattering length densities (electronic densities) are therefore calculated numerically for both X-ray and neutron-scattering densities with the same parameters  $N$  and  $h$ :<sup>6</sup>

$$P(q) = \left( \sum (b_i + 1 - b_i)^4 / 3\pi R_i^3 f(qR_i) \right)^2$$

where

$$f(x) = 3(\sin x - x \cos x)/x^3$$

If the structure is spherical, both X-ray and neutron-scattering spectra can be reproduced on an absolute scale with this single parameter  $\sigma$ . When the calculated scattering cannot be fitted to the observed one by varying  $\sigma$ , at least one of the two underlying assumptions, i.e., (I) the only interaction between droplets is hard-sphere repulsion, and (II) micelles are spherical, has to be modified. For double-chain surfactants, we have recently shown in a similar case that assumption II is wrong.<sup>12</sup>

In the case of glycolipids, the absence of critical points in the phase diagram and no effect of temperature of scattering data shows that it is also merely assumption II which has to be modified: the shape is not spherical. We therefore turn now to the calculation of independent cylindrical micelles. An infinite flexible cylinder is easily detected by a  $q^{-1}$  decay of the scattering. In this case, the scattering is very intense at low  $q$  and it is given by<sup>6</sup>

$$P(q) = (C - C_{\text{cmc}})\pi/qN_1(\bar{b} - b_{\text{solvent}})^2 \exp(-Rg^2q^2/2)$$

Where  $N_1$  is the aggregation number per unit micellar length,  $C$  the concentration,  $C_{\text{cmc}}$  the critical micellar concentration, and  $\bar{b}$  the average scattering length density in the aggregate. The relevant plot  $\log Iq^2$  versus  $\log q$  does not show a linear behavior in the present case.

(8) Jacrot, B.; Zaccari, G. *Biopolymers* 1981, 20, 2413.

(9) Porod G. In *Small Angle X-ray Scattering*; Glatter, Kratky, Eds.; Springer: Berlin, 1982.

(10) Duplessix, R.; Cabane, B.; Zemb, T. *J. Phys.* 1985, 46, 2161.

(11) Hansen, J. P.; Hayter, J. B. *Mol. Phys.* 1982, 46, 651.

(12) Barnes, I. S.; Hyde, S. T.; Ninham, B. W.; Derian, P. J.; Driford, M.; Warr, G. G.; Zemb, T. *Prog. Colloid Polym. Sci.* 1988, 76, 90.

We do not see such signals in our measurements, so we calculate the case of finite cylinders.<sup>13</sup> Other shapes (bilayers, flat disks, etc.) have been considered, but the scattering of them does not correspond either on an absolute scale or qualitatively to the observed shape.<sup>14</sup>

**Model of Finite Cylinders.** We approximate finite spherocylinders made of hydrophobic core coated with a headgroup shell by an elongated ellipsoid (Figure 4). Now, two parameters are required to calculate the whole scattering curve for X-ray and neutron scattering: the area per surfactant headgroup  $\sigma$  and the ellipticity  $e$ . The  $S(q)$  term is set to 1 because no theoretical calculation of  $S(q)$  exists for this case and one does not see sensible decrease of the scattering at low  $q$ , which is the usual indication of steric hindrance.  $P(q)$  is calculated for a prolate ellipsoid of ellipticity  $e$ ; the form factor is given by

$$P(q) = n \left( \sum (b_{i+1} - b_i)^2 \right)^{1/2} / 3\pi R_i^3 f^2 \times (qR_i \sqrt{\cos^2 \theta + e^2 \sin^2 \theta}) \cos \theta d\theta$$

The presence of the ellipticity parameter  $e$  allows solution of the conflict between the surface  $\sigma'$ , which includes all hydrophobic tails, and  $\sigma$ , including the whole surfactant molecule as well as hydration water.

**Polydispersity.** Using small-angle scattering, there is no distinction on a set of scattering data between size and mass polydispersity of the aggregates.<sup>15</sup> But there is a direct way of determination of the variance  $\chi$  of the mass distribution using mass action law and the average mass variation with concentration:

$$\chi^2 = N\delta N / (\delta \ln(x_T - x_1))$$

where  $x_T$  is the total surfactant molar fraction,  $x_1$  the free monomer mole fraction, and  $N$  the aggregation number.

Measurement of mean aggregation number  $N$  for different molar fractions allows therefore the determination of the mass polydispersity of the micelles.

**(2) NMR Techniques.** NMR experiments were performed in the micellar and liquid-crystalline states to get insight into the local organization with special attention toward the local conformation of the polar head.

**NMR in the Micellar State.** All experiments were performed at 310 K using a 24 mM solution in deuterium oxide and a Bruker WM500 spectrometer operating at 500.13 MHz for protons.

In a first stage, all signals arising from nonlabile protons have to be assigned using two-dimensional COSY and multistep Relay experiments.<sup>16</sup> This is facilitated by the fact that anomeric protons from the two glucose units are clearly identified on the spectrum owing to their specific chemical shifts and to coupling constants related to local anomeric characters.

NOE experiments were then carried out to derive spatial proximity between protons and to model the corresponding overall average conformation of the glycolipid molecule.

**NMR in the Liquid-Crystalline State.** When liquid crystals are considered, deuterium NMR offers the most powerful approach to local molecular order and conformation. For this purpose, a deuterium-labeled glycolipid was prepared as follows. Lauric acid was reduced to the corresponding alcohol using Li-AlD<sub>4</sub> and the obtained  $\alpha, \alpha'$ -deuterated dodecanol was grafted to activated maltose using the classical procedures. A 95% labeling of the first carbon of the aliphatic chain was thus achieved. For NMR experiments, all samples were prepared in deuterium-depleted water (CEA) after freeze-drying of the solid glycolipid from this solvent. This ensures that isotropic lines observed in the forthcoming deuterium spectra arise from the labels and not from residual deuterium from the water. All experiments were performed at 310 K using a Bruker MSL300 spectrometer

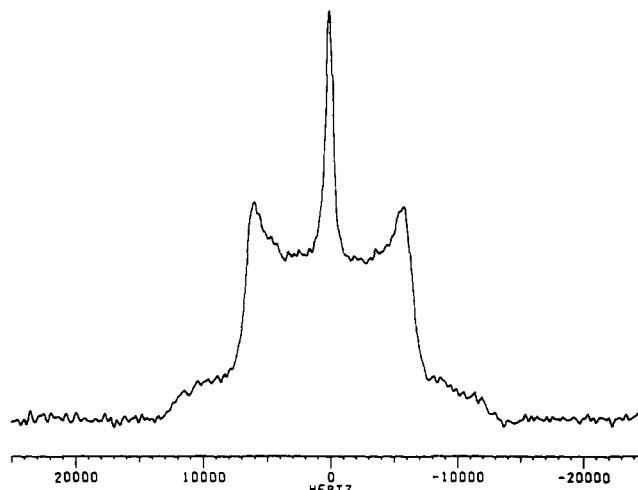


Figure 1. <sup>2</sup>H NMR spectrum of  $\beta$ -dodecyl maltoside in the liquid-crystalline state.

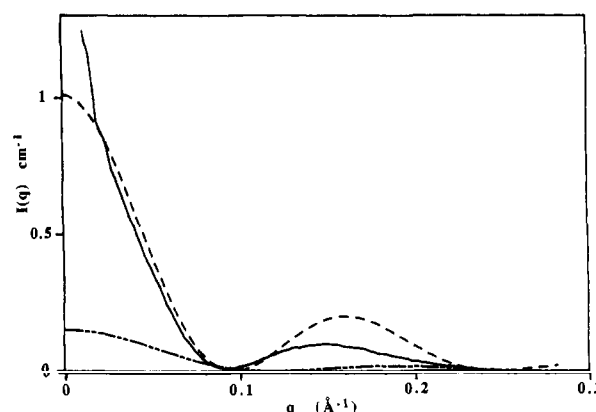


Figure 2. Small-angle neutron scattering observed for a 6% solution of  $\beta$ -C12M in D<sub>2</sub>O compared to the best possible fits for spherical micelles (---) with a fixed area per molecule ( $\sigma' = 0.50 \text{ nm}^2$ ) and short ellipsoids ( $e = 1.2$ ; -.-).

operating at 46 MHz for deuterium. The quadrupolar-echo sequence<sup>17</sup> was used to avoid phase distortions and signal losses.

## Results

**(1) Phase Diagram.** The phase diagram presents only two regions: an isotropic fluid micellar phase exists up to 50% (w/w) in water, and at higher concentration, a viscous birefringent lamellar phase is obtained. The nature of these phases is not affected by temperature up to 353 K. The periodicity  $D^*$  and the thickness  $2t$  of the bilayer are measured by small-angle X-ray scattering at 50%:

$$2t = 2.9 \text{ nm} \quad D^* = 5.3 \text{ nm}$$

The area per surfactant headgroup calculated with these values is therefore  $\sigma = 0.57 \text{ nm}^2/\text{molecule}$ . In the case of lamellar packing,  $\sigma = \sigma'$ .

A typical NMR spectrum in the liquid-crystalline state is displayed in Figure 1. The corresponding 11.4-KHz quadrupolar splitting indicates high molecular ordering at the corresponding carbon, and the overall shape of the spectrum is typical of axially symmetric bidimensional structures. The sharper central line corresponds to isotropically tumbling micelles in thermodynamical equilibrium with the liquid crystals.

**(2) Structure of Micelles.** We study now an aqueous solution of  $\beta$ -dodecyl maltoside (6% w/v) at 310 K: Neutron and X-ray scattering curves are compared on

(13) Hjelm, R. P., Jr. *J. Appl. Crystallogr.* 1985, 18, 452.

(14) Porte, G. *J. Phys. Chem.* 1983, 87, 3541.

(15) Hayter, J. B. In *Proceedings of the XC Corso International School of Physics*; Degiorgio, V., Corti, M., Eds.; North Holland: Amsterdam, 1985.

(16) Berthault, P.; Bossenec, V.; Perly, B. *Analisis*, 1990, 18, i84.

(17) Davis, J. H.; Jeffrey, K. R.; Bloom, M.; Valic, M. I.; Higgs, T. P. *Chem. Phys. Lett.* 1976, 42, 390.

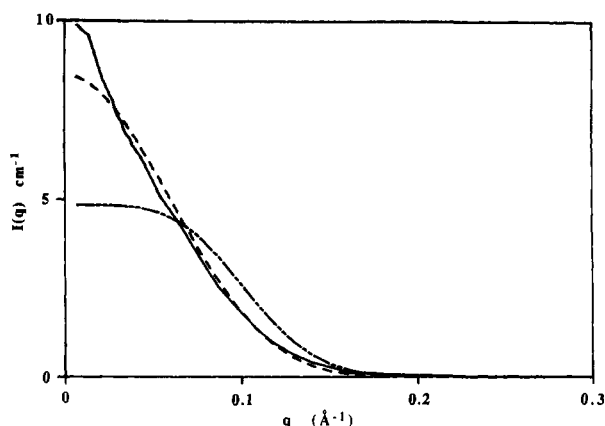


**Figure 3.** Small-angle X-ray scattering of the sample described in Figure 2 compared to the scattering of perfect spheres (---) and short ellipsoids (---). The same numerical values (areas, molecular volumes, aggregation numbers) were used to simulate X-ray and neutron-scattering spectra.

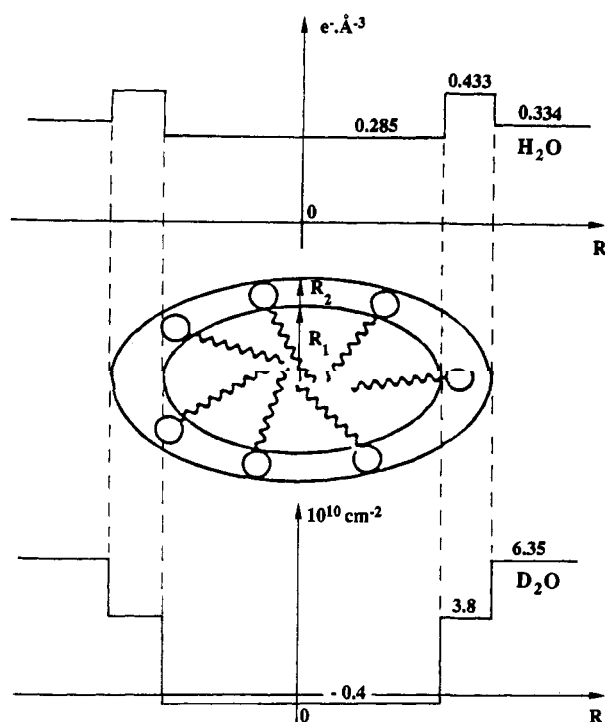


**Figure 4.** Schematic view of the micellar aggregate.

and absolute scale ( $\text{cm}^{-1}$ ) to calculated model curves for spheres and cylinders (Figures 2 and 3). The best result is obtained with the short cylinder model (Figure 4), for both neutron and X-ray techniques, taking the following parameter values:

$$\sigma = 86 \text{ \AA}^2 \quad \sigma' = 51 \text{ \AA}^2$$

which gives an aggregation number  $N = 82$ . Micellar structural parameters are reported in Table II.

A good agreement is not obtained from pure spherical micelles. The short ellipsoid model fits better on the absolute intensity scale. The best agreement is obtained with an ellipticity  $e = 1.2$ . The resulting scattering length density is given in Figure 4.

**(3) Polar Head Conformation.** Anomeric protons were hence used as starting points for the complete assignment of all other signals.

A typical contour plot of a COSY experiment is displayed in Figure 5. The corresponding coupling constants were derived further from computer-assisted spectral simulation. The relevant parameters are reported in Table III.

**Table II.** Structural Parameters Describing the  $\beta$ -Dodecyl Maltoside Micelle at 6% (w/w) in Water at 310 K

$R_2$	total short radius of the micelle	2.4 nm
$R_1$	short radius of the apolar hydrophobic core	1.8 nm
$N$	aggregation number	82
$h$	water molecules per surfactant molecule	10
$e$	ellipticity of the micelle	1.2
$\sigma$	area per surfactant head at the water-micelle interface	$0.87 \text{ nm}^2$
$\sigma'$	area per surfactant head at the chain-headgroup interface	$0.50 \text{ nm}^2$
$b_1$	electronic density of the micellar core	$285 \text{ e nm}^{-3}$
$b_1'$	electronic density of the sugar headgroup region	$433 \text{ e nm}^{-3}$
$b_2$	scattering length density of the micellar core	$-0.4 \times 10^{10} \text{ cm}^{-2}$
$b_2'$	scattering length density of the sugar headgroup region	$3.8 \times 10^{10} \text{ cm}^{-2}$

**Table III.** Chemical Shifts and Coupling Constants of All Protons of the  $\beta$ -Dodecyl Maltoside Polar Head

proton	chem shift, ppm	coupling const, Hz
$H_1$	5.30	$J_{1-2} = 4.2$
$H_2$	3.60	
$H_3$	3.65	$J_{2-3} = 8.7$
$H_4$	3.40	$J_{3-4} = 10.0$
$H_5$	3.65	$J_{4-5} = 9.4$
$H_6-H_6'$	3.80	$J_{5-6} = 4.0, J_{6-6'} = -12.4$
$H_1'$	4.35	$J_{1-2} = 8.3$
$H_2'$	3.35	
$H_3'$	3.70	$J_{2-3} = 8.5$
$H_4'$	3.65	$J_{3-4} = 9.0$
$H_5'$	3.45	$J_{4-5} = 8.5$
$H_6'-H_6''$	3.80	$J_{6-6'} = -12.4$

**Table IV.** Structure of the Micelles for Different Surfactant Concentrations<sup>a</sup>

concn (w/w), %	aggregation no. $N$	$\phi$	$R_1$	$R_2$	$e$
1	120	0.014	21	36	1.2
4	115	0.056	21	36	1.2
6	82	0.084	18	24	1.2

<sup>a</sup>  $e$  is the ellipticity for which the best fit was achieved.  $R_1$  and  $R_2$  are the hydrophobic core radius (short axis) and the external radius, respectively. The excluded-volume fraction  $\phi$  includes 10 water molecules per headgroup.

A two-dimensional NOESY experiment was performed with 150-ms mixing time. The corresponding contour plot is displayed in Figure 6 and shows a number of structure-related cross-peaks. More accurate quantitative data were then obtained by NOE experiments using the buildup technique. NOE buildup rates were obtained at variable transfer times, and these rates could then be converted into effective interproton distances. A complete rationalization of all data was achieved using a molecular modeling program,<sup>18</sup> allowing proposal of a model for a single glycolipid molecule in the micelle. In these calculations, a normal  ${}^4C_1$  chair conformation was used for both sugar units in agreement with coupling constants. Only the interglycosidic and the glycosidic bonds were considered for local rotation. The relevant molecular structure is depicted in Figure 7.

## Discussion

The extended chain length for the  $\beta$ -dodecyl maltoside is  $L_c = 1.8 \text{ nm}$ ;<sup>10</sup> The apolar volume of this chain is  $V_c = 0.315 \text{ nm}^3$ . Therefore, the maximum aggregation number of a spherical apolar core without a hole at the center corresponds to  $N = 82$ , when  $R_1 = L_c$  and  $\sigma = 0.50 \text{ nm}^2$ .

(18) Langlet, G. 44<sup>ème</sup> Réunion Internationale de modélisation des structures et propriétés moléculaires en chimie physique et biophysique, Nancy, France, 1989.

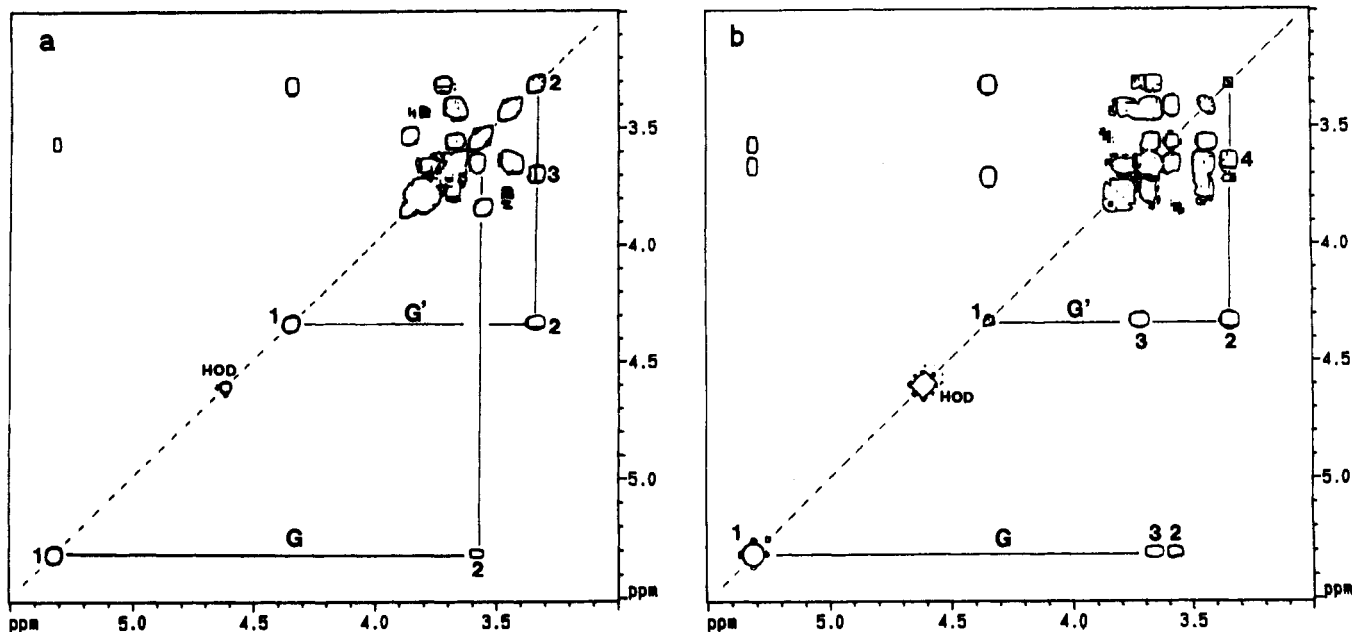


Figure 5. Partial 500-MHz contour plots of COSY (a) and single Relay (b) experiments.

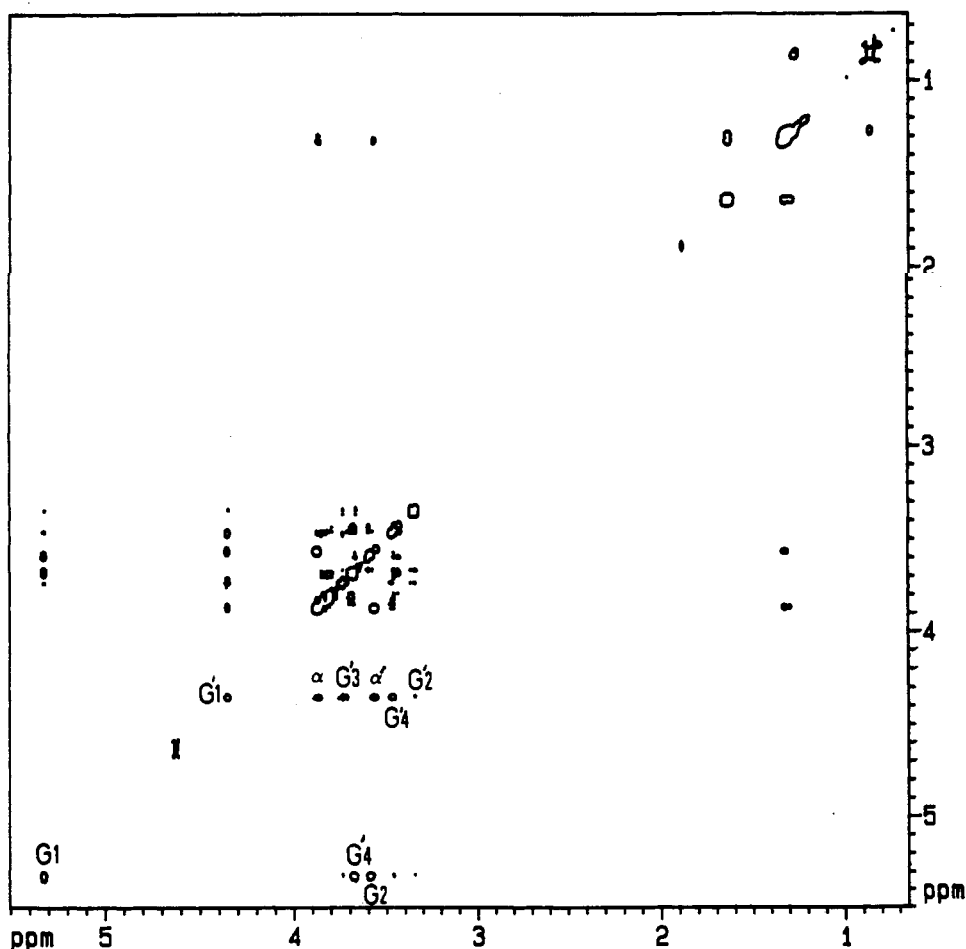


Figure 6. Contour plot of a phase-sensitive NOESY experiment (150-ms mixing time). Only negative levels are plotted.

The size of the extended maltoside headgroup is  $R_h = 1.2$  nm, and the maximum radius  $R_2$  is  $R_2 = L_c + R_h = \text{ca. } 3$  nm. In the present case, the external radius of the micelle is 24 Å along the small axis and 28 Å along the long axis, allowing enough room for the sugar headgroups and also satisfying the conditions of occupancy of the center of the micelle; i.e., (a)  $L_c \geq R_1$  and (b)  $eR_2 = L_c + L_h$ . When the long axis reaches 30 Å, linear growth of the micelle stops.

When there is no stopping mechanism for micellar

growth, infinite cylindrical micelles are formed.<sup>14</sup> In our case, the cylindrical structure is forbidden by the volume of the headgroup, as it should require dehydration of the sugar polar head. The micelle hence grows toward an ellipsoid but cannot reach the cylindrical state. Experimentally, there is no way to fit the scattering with the expressions of the scattering of cylindrical micelles.

The ellipsoid length is limited to the length of the extended molecule (3 nm). The two constraints inducing

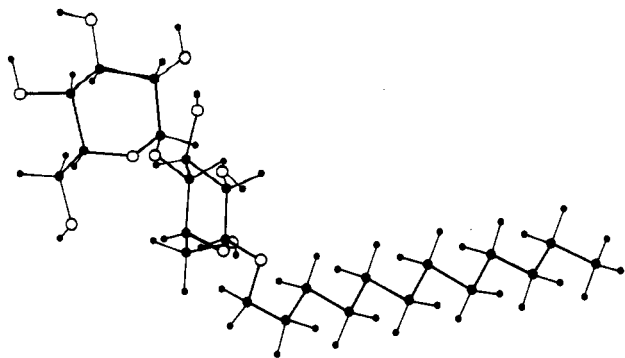


**Figure 7.** Schematic lateral view of the polar headgroup conformation.

the ellipsoidal shape are as follows: (a) the area at the chain-headgroup interface  $\sigma = 0.5 \text{ nm}^2$ ; this fixes the maximum value of  $R_1$ . (b) The total headgroup volume between  $R_1$  and  $R_2$  has to include the  $2N$  hydrated sugar cycles; this induces an ellipsoidal shape. These two geometrical conditions are satisfied by the prolate ellipsoidal shape of the glycolipid micelle.

From the observed scattering alone, one could also invoke size polydispersity of micelles instead of a distribution of monodisperse ellipsoids, as this will yield similar scattering curves. An independent evaluation of polydispersity is however provided by the variation of the average aggregation number with concentration.<sup>6</sup> Table IV gives the aggregation numbers at three concentrations.

The lack of variation of these numbers with concentration implies that polydispersity should be lower than a few percent. As this value is too small to explain the scattering curves, a shape deformation has to be invoked instead of a contribution of polydispersity.

### Conclusion

The two sterical constraints responsible for the shape of the micellar aggregate are strongly dependent on the sugar ring conformation and orientation relative to the chain-headgroup interface plane. Therefore, interaction of the sugar head with any other molecule such as a protein can dramatically change the value of  $\sigma'$  when the sugar conformation or orientation changes. The value of  $\sigma'$  can easily increase by a large factor (up to 3) when the ring lies parallel to the interface. This should strongly decrease the size of the micelle. Along the same idea, when the glycolipid is mixed with another surfactant, as in biological membranes, the spontaneous curvature toward oil should decrease drastically. This is also a possible mechanism for inhibiting the decrease of the radius of gyration if binding of a protein can induce headgroup conformation changes. This mechanism is now under investigation using mixed glycolipid-ionic surfactant mixed micelles.

**Acknowledgment.** We are grateful to Dr. C. Williams (Lure, Orsay), to Dr. L. Auvray (Laboratoire Léon Brillouin, CEA Saclay), and to G. Langlet (SCM, CEA Saclay).